Prostate Tumor Identification in Ultrasound Images

Chuan-Yu Chang[1], Meng-Yu Tu[1], and Yuh-Shyan Tsai[2]

[1] Department of Computer Science and Information Engineering,
National Yunlin University of Science and Technology, Yunlin, Taiwan
[2] Department of Urology, National Cheng Kung University Hospital, Tainan, Taiwan
chuanyu@yuntech.edu.tw

Abstract. There are various medical imaging instruments used for diagnosing prostatic diseases. Ultrasound imaging is the most widely used tool in clinical diagnosis. Urologist outlines the prostate and diagnoses lesions based on his/her experiences. This diagnostic process is subjective and heuristic. Active contour model (ACM) has been successfully applied to outline the prostate contour. However, application of ACM in outlining the contour needs to give the initial contour points manually. In this paper, an automatic prostate tumor identification system is proposed. The sequential floating forward selection (SFFS) is applied to select significant features. A support vector machine (SVM) with radial basis kernel function is used for prostate tumor identification. Experimental results showed that the proposed method achieved higher accuracy than those of other methods.

Keywords: prostate tumor, feature selection, support vector machine.

1 Introduction

The prostate is a compound tubuloalveolar exocrine gland of the male reproductive system in most mammals. Prostate cancer has been the fifth most common malignancy and the seventh leading cause of cancer deaths in Taiwan. More than 3,000 men are diagnosed annually with prostate cancer, of which approximately 1000 die. Prostate cancer has become a common male urinary tract cancer.

Prostate is located in the pelvis, below the bladder and before the rectum. Most of the early prostate cancers have no symptoms, it's often discovered during routine health examination. Prostate specific antigen (PSA) blood test and digital rectal examination of the prostate are methods for prostate cancer screening. In order to detect early prostate cancer, physicians usually apply the ultrasound imaging to visualize prostate for diagnosis if either elevated PSA or abnormal Digital Rectal Examination (DRE). However, diagnosis by DRE is very subjective and highly depending on the experiences of urologist.

Various imaging modalities, such as magnetic resonance imaging (MRI), computerized tomography (CT), and ultrasound (US) imaging, are widely used in the diagnosis of various diseases with the assistance of medical image analysis techniques. In which, US imaging is inexpensive, non-invasive, and easy to use. Thus,

J.-S. Pan et al. (eds.), *Intelligent Data Analysis and Its Applications*, *Volume 2*,
Advances in Intelligent Systems and Computing 298,
DOI: 10.1007/978-3-319-07773-4_2, © Springer International Publishing Switzerland 2014

ultrasound images become the most commonly used in clinical diagnosis, such as inspecting the prostate[4,6,7,8], breast tumor[3] and thyroid nodule[2].

Physician have outlined prostate region in ultrasound image when clinical diagnosis, and then determine whether a tumor within the region, outlined tumor area for tumor diagnosis. However, outlining the tumor area in ultrasound images is highly relied on physicians' experiences, it's inefficient and subjective. Therefore, we proposed a prostate tumor identification system in ultrasound images is proposed in this paper.

This paper is organized as follows: Section 2 presents the proposed prostate tumor identification method. Experimental results are presented in Section 3, where we compared with other method. Conclusions are drawn in Section 4.

2 Proposed Method

In this paper, an automatic SVM-based prostate tumor identification in ultrasound images is proposed. First, a preprocessing is adopted to reduce the influence of speckle noise and therefore enhance the contrast of prostate region. Second, a total of 236 features are extracted from each ROI. Third, the sequential floating forward selection (SFFS) is applied to select significant features. Finally, a support vector machine (SVM) with radial basis kernel function is used for prostate tumor identification. Figure 1 shows the flow diagram of the proposed method. Details of the procedures are described in the following subsections.

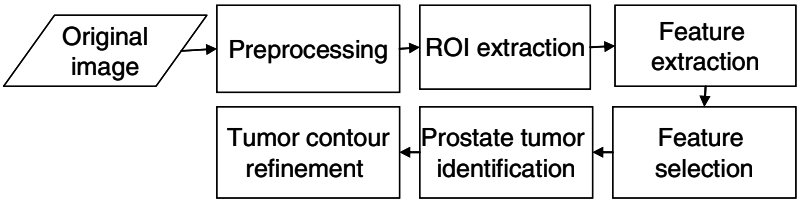

Fig. 1. Flow chart of the proposed method

2.1 Preprocessing

Since speckle noise and poor contrast in ultrasound images will affect the identification accuracy of the prostate tumor. Hence, speckle reduction by means of digital image processing should improve image quality and possibly the diagnostic potential of medical ultrasound.

In this paper, a 5×5 average filter [7] is used to reduce inevitable speckle noise in the prostate ultrasound images. A power-law [7] transformation is then applied to enhance the contrast; parameters c and r of power-law transformation are set as 1 and 0.7, respectively. Figure 2 shows the result of preprocessing. After preprocessing we can clearly see that the contrast between the prostate and background was strengthened.

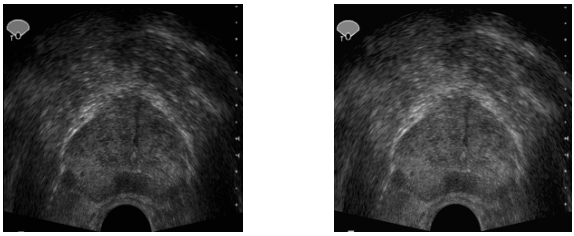

(a) (b)

Fig. 2. (a) original image, (b) result after preprocessing

2.2 ROI Extraction

In order to identify the prostate tumor in the ultrasonic images, a lot of ROIs includes prostate tumor and non-tumor were outlined by an experienced urologist and confirmed by biopsy. Based on the sliding-windows method, a block with size of 23×23 is sliding on the outlined ROIs to segment patterns of tumor and non-tumor. The blocks are arrayed adjacent to each other with an $M\times M$ overlap. Figure 3 shows a case of outlined prostate tumor in ultrasound image. The extracted normal and tumor patterns are showed in Fig. 3(b) and (c), respectively.

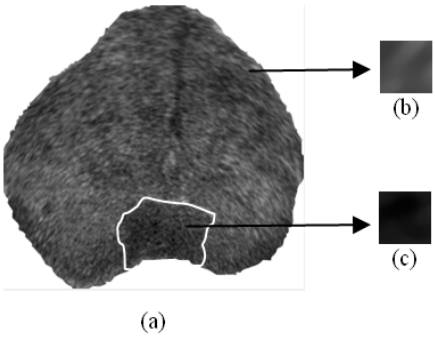

Fig. 3. (a) prostate region, (b) normal prostate pattern, (c) prostate tumor pattern

2.3 Feature Extraction

Textural features contain important information that is used for analysis and explanation of US images. In this paper, 236 features were extracted from the selected ROIs. Features are calculated from 11 different textural matrixes and transformations namely graylevel co-occurrence matrix (GLCM), Statistical Feature Matrix, Gray Level Run-Length Matrix, Laws' Texture Energy Measures, Neighboring Gray Level Dependence Matrix, Haar wavelet, homogeneity, histogram, block difference of inverse probabilities (BDIP) [10], Discrete Cosine Transform, and normalized multi-scale intensity difference (NMSID) [11].

2.4 Feature Selection

In previous stages, 236 features are obtained from each ROI. We can simply use them to identify prostate tumor, but it will be time-consuming. Feature selection is a common way to improve this situation. The sequential floating forward selection (SFFS) is adopted to sift significant features. The SFFS method consists of Sequential Forward Selection (SFS) and Sequential Backward Selection (SBS), which are capable of correcting wrong inclusions and removal decisions. Figure 4 shows the flow diagram of SFFS.

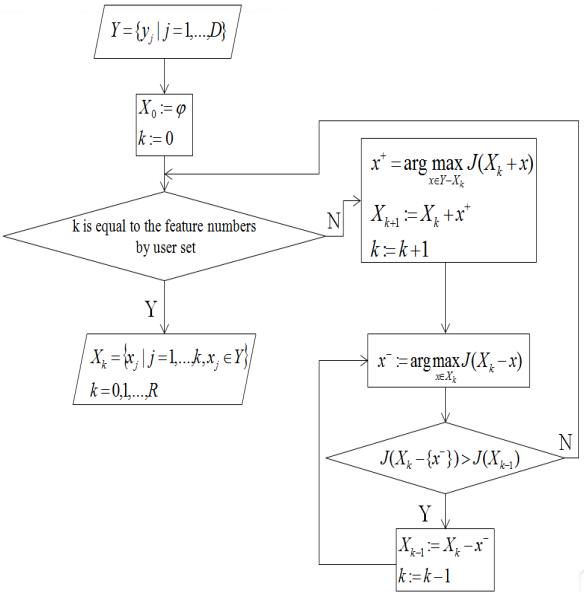

Fig. 4. The flow diagram of SFFS

In which, Y is features for all groups, D is the number of feature item, X is the best feature set selected from Y, R is the numbers of X, $J(x)$ is the cost function that evaluate the classification accuracy of feature set X. The terminative condition of the SFFS algorithm is the number of features k. The SFFS algorithm is summarized as follows:

Step 1: Input a feature group Y and set the terminative condition k.
Step 2: Use the function $J(x)$ to evaluated Y, that we can obtained a best feature x^+, then put the x^+ into the best feature group X.
Step 3: Use the function $J(x)$ to evaluated X to obtain a best feature x^-.
Step 4: Compared the best feature set without x^- ($J(X_k - x^-)$) and the best feature set of previous, if $J(X_k - x^-)$ is bigger than the best feature set of previous, then the best feature set of previous is equal to the best feature set without x^-, and k minus one then return to step 3. If $J(X_k - x^-)$ is not bigger than the best feature set of previous, then return to step 2 until reached the stop condition.

After the SFFS, five representative features were selected. Among them, four features are extracted from GLCM and one is extracted from textural energy matrix. The details of the selected features are described as follows:

The sum average of gray level co-occurrence matrix (GLCM) is defined as:

$$Sum\ Average = \sum_{i=2}^{2L} i p_{x+y}(i) \cdot \tag{1}$$

$$p_{x+y}(k) = \sum_{i=0}^{L} \sum_{\substack{j=0 \\ i+j=k}}^{L} p(i,j), \quad k = 2,3,...,2L \cdot \tag{2}$$

where L is the largest grey value in the image.

The contrast of gray level co-occurrence matrix (GLCM) is defined as:

$$Contrast = \sum_{n=0}^{L} n^2 \left(\sum_{i=0}^{L} \sum_{\substack{j=0 \\ |i-j|=n}}^{L} p(i,j) \right) \cdot \tag{3}$$

$p(i,j)$ is the values from gray level co-occurrence matrix after normalized, it defined as:

$$p(i,j) = \frac{C(i,j)}{\sum_{i,j} C(i,j)} \cdot \tag{4}$$

where $C(i,j)$ is the values of gray level co-occurrence matrix coordinate (i,j).

The difference entropy of gray level co-occurrence matrix(GLCM) is defined as:

$$Difference\ Entropy = -\sum_{i=0}^{L} p_{x-y}(i) \log\left(p_{x-y}(i)\right) \cdot \tag{5}$$

$$p_{x-y}(k) = \sum_{i=0}^{L} \sum_{\substack{j=0 \\ |i-j|=k}}^{L} p(i,j), \quad k = 0,1,...,L \cdot \tag{6}$$

The difference variance of gray level co-occurrence matrix (GLCM) is defined as:

$$DifferenceVariance = \sum_{i=0}^{L} \left(i - \sum_{j=0}^{L} j p_{x-y}(j) \right)^2 p_{x-y}(i) \cdot \tag{7}$$

In the present study, Law's texture energy [5] computed through the following two masks are used to obtain the texture features:

L5 (Level) = [1 4 6 4 1]

S5 (Spot) = [-1 0 2 0 -1]

The L5 vector gives a center-weighted local average. The S5 vector detects spots. In this study, a 2D convolution masks, namely S5L5 is obtained by computing the

outer products of pairs of 1D masks. By convoluting the image with the 2D mask, a texture energy maps are acquired. The statistics mean of the texture energy maps is then calculated and used as the texture feature.

2.5 Prostate Tumor Identification

Support vector machine (SVM) is a supervised classifier and it has been widely used in regression analysis and statistical classification. The basic idea of SVM is to map the input data into a high-dimensional feature space, and find the hyperplane that maximizes the margin between two classes. Fig. 5 shows the schematic of hyperplane. A SVM is used to identify the prostate tumor. In this paper, the SVM was implemented using the LIBSVM [1], and the radial basis function (RBF) defined as Eq.(8) was selected as the kernel function.

$$K(x^{(s)}, x_i) = \exp\left(\frac{-\left\|x^{(s)} - x_i\right\|^2}{2\sigma^2}\right). \tag{8}$$

where σ^2 is the width of the kernel.

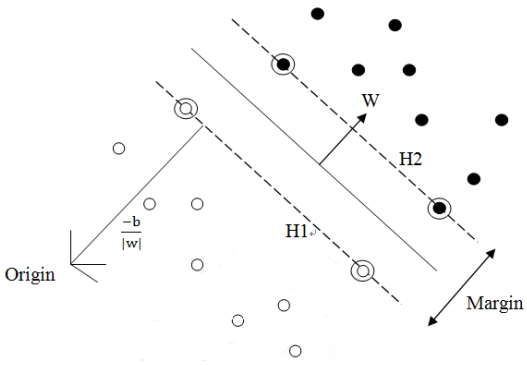

Fig. 5. Schematic concept of hyperplane

2.6 Tumor Contour Refinement

The above procedures can almost segment the prostate tumor completely. However, there still existed some artifact may be classified as part of prostate tumor. A morphological technique is utilized to separate the artifacts from a prostate tumor. Erosion with a 17×17 structuring element is derived to remove the connection between artifacts and prostate tumor. A region filling is then applied to fill holes in tumor region. Finally, dilation with a 17×17 structuring element is performed to recover the original size. The largest region is viewed as the tumor region.

3 Experimental Results

To show the capacity of the proposed method, the prostate ultrasound images for these experiments were taken at the urology department of National Chen Kung University Hospital. Resolution of the image is 3200×2400. A total of 35 cases were used in our experiments. In which, ten cases were chosen as training samples and the remaining cases were chosen as testing samples. The prostate tumor identification system was implemented by Microsoft Visual C# 2008 on a PC with 3.40 GHz Intel Core i7-2600 processor and 4GB RAM.

3.1 Preprocessing

The objective of the preprocessing is to reduce the influence of speckle noise and enhance the contrast of original ultrasound images. Figure 6 shows the results after preprocessing. The left column of Fig. 6 shows original ultrasound images. The results after the preprocessing were showed in the right column of Fig. 6. Obviously, after preprocessing we can clearly see that the contrast between the prostate and background was strengthened.

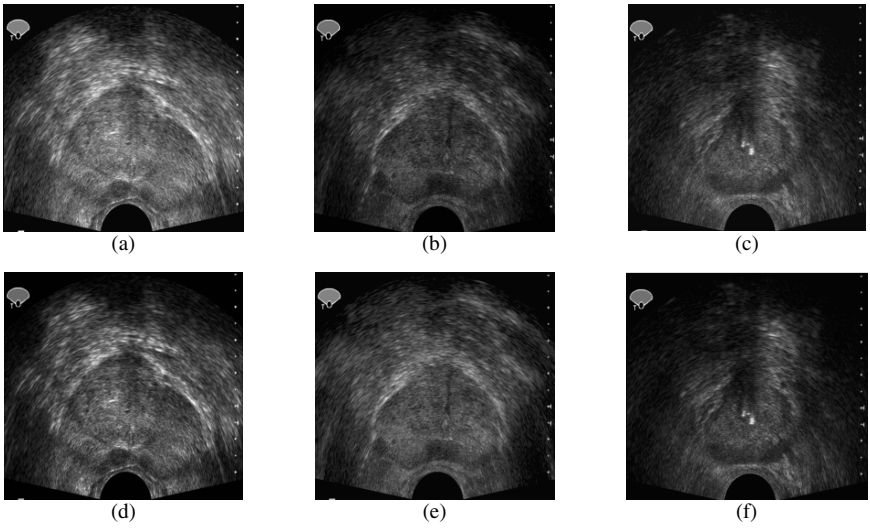

Fig. 6. (a-c) original prostate ultrasound image, (d-f) results after pre-processing

3.2 Prostate Segmentation and Tumor Classification

Before urologists diagnose prostate lesions, the contour of the prostate in US images must be manually outlined. However, manual segmentation is a time-consuming and non-reproducible task. Thus, an automatic prostate segmentation system combines the active contour model (ACM) is adopted [12]. The prostate classifier consists of a validation incremental neural network (VINN) and a radial-basis function neural network (RBFNN). Figure 7 shows the results of outlined the region of prostate in

ultrasound images. Obviously, the prostate region is correctly outlined. Figures 8(a, c, e) show the results of prostate tumor identification. There are many holes existed in prostates. Figures 8 (b, d, f) show the refinement results of Fig. 8 (a, c, e). The holes were removed, and prostate tumors were correctly outlined.

Figure 9 shows the prostate tumor identification results of the proposed method and outlined by urologist manually. Obviously, the outlined tumors of the proposed system are very close to the results outlined by experienced urologist.

(a) (b) (c)

Fig. 7. The outlined prostates in ultrasound images. (a) case1, (b) case2, (c) case3.

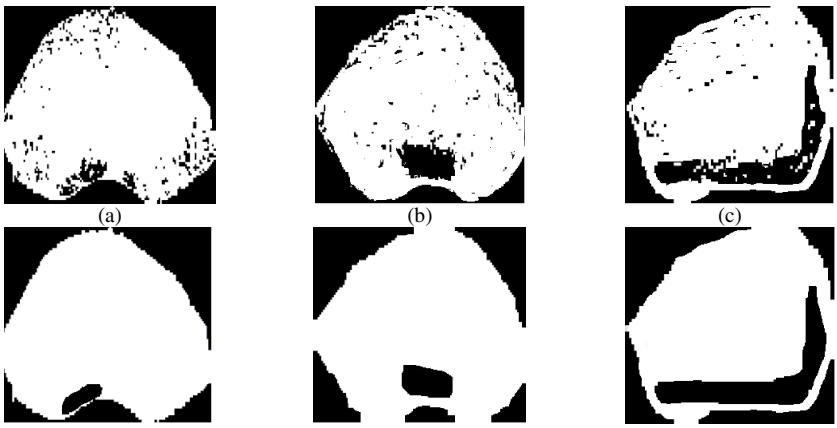

(a) (b) (c)

(d) (e) (f)

Fig. 8. (a-c) The results after prostate tumor identification. (d-f) The results after prostate tumor refinement.

3.3 Accuracy Evaluation of Prostate Tumor Segmentation

For a fair comparison, the accuracy was used to quantify the performance. Accuracy is defined as follow:

$$Accuracy = (N_{tp} + N_{tn}) / (N_p + N_n). \tag{9}$$

where N_p is the total number of pixels of the tumor, N_n is the total number of pixels of non-tumor region, N_{tp} is the number of actual prostate tumor detected by the proposed method, N_{tn} is the number of actual non-tumor pixels detected as

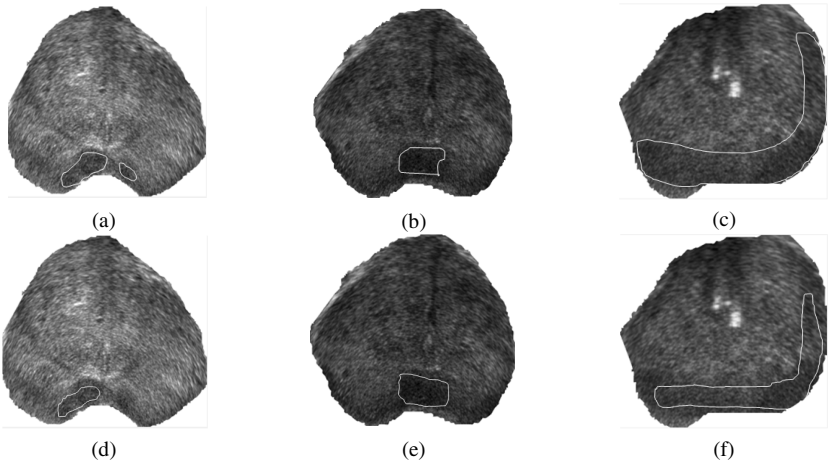

Fig. 9. (a-c)physician outlined tumor, (b-f) outlined tumors of the proposed method

non-tumor pixels, N_{fn} is the number of system classification as the non-tumor region in physician outlined tumor region, N_{fp} is the number of actual non-tumor pixels detected as tumor pixels.

To demonstrate the accuracy of the proposed method is higher than that of Zhang's method [9], Table 1 shows the comparison results. The accuracy of the proposed and Zhang's methods are 91.58% and 90.54%, respectively.

Table 1. Accuracy of Zhang's and proposed method

	The proposed method	Zhang's method
Accuracy	91.58%	90.54%

Table 2. The result for differential parameter

ROI size	Filter size	# of the best feature set	Accuracy
17×17	3×3	6	89.4%
17×17	5×5	5	87.67%
17×17	7×7	6	87.04%
19×19	3×3	7	89.08%
19×19	5×5	6	88.3%
19×19	7×7	6	87.06%
21×21	3×3	4	88.24%
21×21	5×5	5	89.49%
21×21	7×7	6	85.53%
23×23	3×3	4	91.56%
23×23	5×5	5	93.45%
23×23	7×7	6	91.85%
25×25	3×3	4	90.88%
25×25	5×5	5	91.74%
25×25	7×7	5	90.88%

3.4 Determination of ROI Size and Denosing Filter Size

To achieve a high accuracy, the size of ROI, masks, and the number of selected features should be appropriately set in the testing procedure. In order to obtain the appropriate parameters, various ROI sizes and denosing filter sizes were performed. Table 2 shows the accuracies for different parameters. The highest accuracy is achieved when the size of ROI and size of filter is set to 23×23 and 5×5, respectively.

4 Conclusion

In this paper, we proposed a SVM-based method for identification of prostate tumor in ultrasound images. The system can assist urologists on clinical diagnosis. The representative features after feature selection can save lots of time in classification and improve the classification results. According to the experimental results, the average accuracy rate has reach 91.58%. Our experiments have better accuracy than Zhang's method.

Acknowledgments. This work was supported in part by the by the National Science Council Taiwan, R.O.C, under the grants NSC 100-2628-E-224-003–MY3.

References

1. Chang, C., Lin, C.: LIBSVM: a library for support vector machines, 2.91. ed: Citeseer (2001)
2. Maroulis, D.E., Savelonas, M.A., Iakovidis, D.K., Karkanis, S.A., Dimitropoulos, N.: Variable Background Active Contour Model for Computer-Aided Delineation of Nodules in Thyroid Ultrasound Images. IEEE Trans. Infor. Tech. in Biomed. 11, 537–543 (2007)
3. Chen, D.R., Chang, R.F., Wu, W.J., Moon, W.K., Wu, W.L.: 3-D breast ultrasound segmentation using active contour model. Ultrasound in Medicine and Biology 29, 1017–1026 (2003)
4. Sahba, F., Tizhoosh, H.R., Salama, M.M.: Application of Reinforcement Learning for Segmentation of Transrectal Ultrasound Images. BMC Medical Imaging, 1471–2342 (2008)
5. Laws, K.: Textured image segmentation. University of southern california, Los Angeles Image Processing Institute (1980)
6. Betrouni, N., Vermandel, M., Pasquier, D., Maouche, S., Rousseau, J.: Segmentation of Abdominal Ultrasound Images of the Prostate Using a Priori Information and an Adapted Noise Filter. Computerized Medical Imaging and Graphics, 43–51 (2005)
7. Gonzalez, R.C., Woods, R.E.: Digital Image Processing, 2nd edn. (1992)
8. Mohamed, S.S., Salama, M.M.: Spectral Clustering for TRUS Images. BioMedical Engineering OnLine (2007)
9. Zhang, Y., Sankar, R., Qian, W.: Boundary delineation in transrectal ultrasound image for prostate cancer. Comp. Biol. Med., 1591–1599 (2007)
10. Chum, Y.D., Seo, S.Y.: Image Retrieval using BDIP and BVLC Moments. IEEE Transactions on Circuits and Systems for Video Tech. 13, 951–957 (2003)
11. Chen, E.L., Chung, P.C., Chen, C.L., Tsai, H.M., Chang, C.I.: An automatic diagnostic system for CT liver image classification. IEEE Trans. on Biomedical Engineering 45, 783–794 (1998)
12. Chang, C.Y., Tsai, Y.S., Wu, I.L.: Integrating Validation Incremental Neural Network and Radial-Basis Function Neural Network for Segmenting Prostate in Ultrasound Images. International Journal of Innovative Computing, Information and Control 7, 3035–3046 (2011)